Biomaterials and Biomechanics in Bioengineering, *Vol. 5, No. 1 (2020) 25-35*
DOI: https://doi.org/10.12989/bme.2020.5.1.025

Approximated 3D non-homogeneous model for the buckling and vibration analysis of femur bone with femoral defects

Saleh Mobasseri*[1], Mehdi Sadeghi[1], Maziar Janghorban[1] and Abdelouahed Tounsi[2]

[1]*Department of Mechanical Engineering, Marvdasht Branch, Islamic Azad University, Marvdasht, Iran*
[2]*Material and Hydrology Laboratory, Faculty of Technology, Civil Engineering Department, University of Sidi Bel Abbes, Algeria*

(Received June 29, 2018, Revised February 24, 2020, Accepted March 12, 2020)

Abstract. We carry the knowledge that the skeleton bones of the human body are not always without defects and some various defects could occur in them. In the present paper, as the first endeavor, free vibration and buckling analysis of femur bones with femoral defects are investigated. A major strength of this study is the modeling of defects in femur bones. Materialise Mimics software is adopted to model the bone geometry and the SOLIDWORKS software is used to generate the defects in bones. Next, the ABAQUS software is employed to study the behaviors of bones with defects.

Keywords: femur bone; femoral defects; 3D non-homogeneous model; free vibration; buckling

1. Introduction

Femur bone is the largest and longest bone found in the human body (Gupta and Tse 2014). The femur bone plays an important role in the weight of body (Jade 2012). It has strong potential for fracturing in comparison with other bones, especially for the elderly people (Gupta and Tse 2014). The hip joint is constructed with the connection of proximal end of femur bone to the pelvis and the knee joint is formed with the connection of tibia to the distal end of femur bone (Jade 2012). Up to now several works have been studied the behaviors of femur bones (Hambli 2014, Yosibash *et al*. 2014, El Sallah *et al*. 2016). Kumar *et al*. (2014) studied the femur bone with no defects using the simulation software based on the finite element method to find out the modes of vibration, the natural frequencies and the location of bone fracturing. Voo *et al*. (2004) presented a methodology for investigating stress fracture injuries using computational models and biomechanical stress analysis in a human femur bone. It was concluded that certain geometric features are important risk factors for the stress fracture of femoral neck. Haider *et al*. (2013) developed a QCT-derived FE model of a proximal femur including node-specific modulus assigned on the basis of local bone density. According to an applied fracture load, the influences of three commonly used boundary conditions available in literature were investigated with the comparison of resulting strain field. Bending analysis of femur bones was done by Bhardwaj *et al*. (2014) to find out the mechanical behaviors of them by using FE software. In their work, Von Mises and bending stresses were calculated for a known critical load. It was obtained that the maximum Von Mises stresses were about 131.3 MPa,

*Corresponding author, M.sc., E-mail: saleh.mobasseri@gmail.com, saleh.mobasseri@miau.ac.ir

http://www.techno-press.org/?journal=bme&subpage=8 ISSN: 2465-9835 (Print), 2465-9959 (Online)

and the maximum deflection was calculated to be 1.8 cm, for the critical bending moment of 200 N.m. In order to find the way to determine the orthotropic properties in a proximal femur, (San *et al*. 2012) suggested a finite element model based on the directions of the principal stresses produced by a physiological load scheme. To study the effects of material properties on the mechanical behaviors of bone in their suggested method, isotropic and orthotropic models were chosen. Taylor *et al*. (2002) CT scanned a cadaveric bone to calculate the natural frequencies by adopting a modal analysis. After modeling the geometrical shape of bone, a FE model was constructed and the maximum values of the orthotropic elastic constants were achieved by comparing the results of this model with those obtained from the experimental test. Geraldes and Phillips (2014) presented an iterative orthotropic three-dimensional adaptation algorithm for a FE model of the whole femur bone. The orthotropic prediction for the material properties of femur bone leads to the better prediction for the density of bone in comparison with the isotropic approach. The inaccuracy of isotropic models is also investigated in present paper, which will be discussed in the next sections. Nishiyama *et al*. (2013) developed a fast and validated methodology to predict the structural stiffness of bone and its failure load with a sensitivity study of varying boundary conditions. The effects of age-related differences in femoral loading and bone mineral density on strains were investigated by Anderson and Madigan (2013). They concluded that by decreasing bone mineral density, strains in a fairly uniform manner will increase. Campion *et al*. (2017) investigated a below-knee amputation based on a new finite element method for the optimization of prosthesis shape. Belaid *et al*. (2017) studied mechanical behavior of stabilization techniques for tibial plateau fractures by applying finite element method. In their work, displacements and stresses related to the fracture were presented. The effects of real complex bone geometry on natural frequencies were studied by Sadeghi *et al*. (2018). Stability of the distal femoral defect after reconstruction with fibular grafts of different lengths were analyzed by Ma *et al*. (2014) in which a three-dimensional model of a healthy volunteer was developed using computed tomography images. Biomechanical performance of the metal plate and bone strut technique for fixing recalcitrant nonunion of femur midshaft segmental defects was reported by Coquim *et al*. (2018). The effect of initial stress and magnetic field on the behavior wave propagation in human dry bones were studied by Mahmoud *et al*. (2014).

In present article, free vibration and buckling analysis of femur bone with femoral defects are studied for the first time. Different types of femoral defects are considered to calculate the natural frequencies, critical buckling loads and modes of vibration and buckling. Moreover, according to the real behaviors of bones, a possible better model for the material properties of femur bones in comparison with some other works is also presented. With considering our results, it can be found that present 3D models may proof the inaccuracy of isotropic models for both healthy femur bones and femur bones with femoral defect. At the end of this section, it is mentioned that the idea presented in this article about non-homogeneous model has a good potential to be investigated from different views. For example, one can check that whether this model is more accurate than isotropic model or not. In which topics it has more accuracy and in which one it is not applicable? Moreover, other analyses such as forced vibration or impact can be done based on present models.

2. Femoral defect

In daily life, the human body undergoes some vibrations, for example, the exerted vibrations on the automobile passengers as a result of the road speed bumps. On the other hand, buckling can also be occurred to our body because of several different compression loads that may be exerted to our

Fig. 1 Femoral defect (Amanatullah *et al*. 2014): 17% cortical defect (A), 33% cortical defect (B), 50% cortical defect (C), and 67% cortical defect (D)

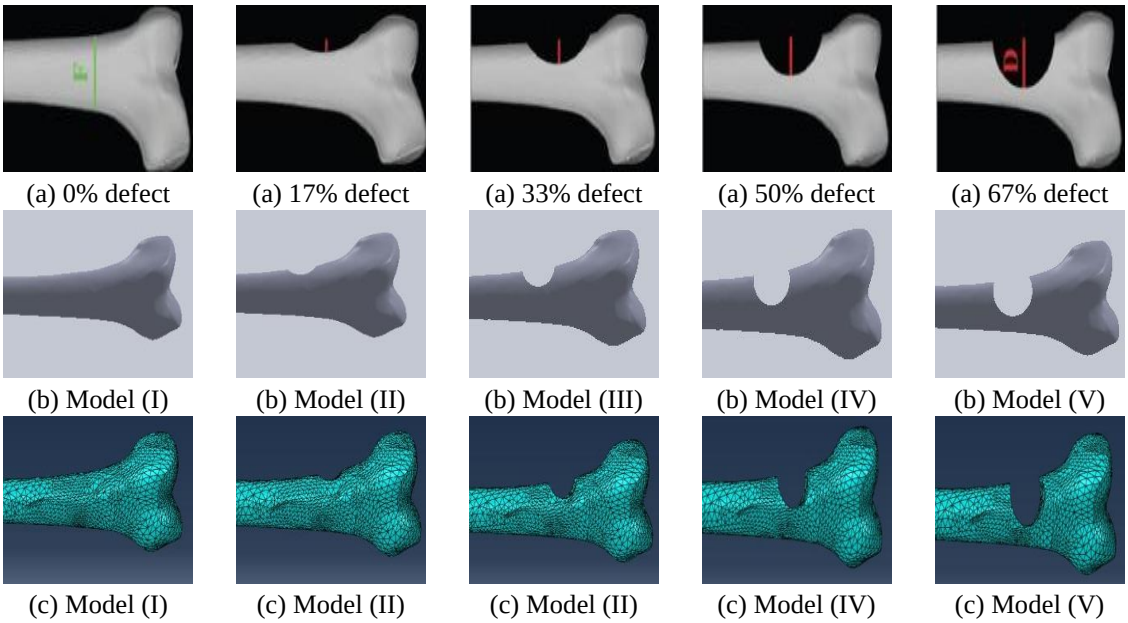

Fig. 2 (a) Computer tomographic reconstruction of each femoral defect (Amanatullah *et al.* 2014), (b) Approximated models for different types of defects, (c) Meshed models for different types of defects

bones. Besides, in real life, skeleton bones are not always healthy with no defects and several different factors can cause bone damage. Regarding the mentioned descriptions, it seems that the inspection of the bone's vibrations and buckling in the presence of the defects would be necessary and valuable research.

In Fig. 1, different types of femoral defects in real femur bones are introduced. In this figure, cortical defect percent is determined by dividing the maximal depth of resection by the width of the femur at that location Amanatullah *et al*. (2014). These defects can be also seen in part (a) of Fig. 2. More information on the size of defects and their geometries were defined by Amanatullah *et al*. (2014). It is noted that cortical bone is made up of a solid external layer throughout the walls of the diaphysis and the external surfaces of bone while cancellous bone, is located in the epiphyseal and metaphyseal region of long bones and has 30 percent greater porosity than cortical bone (Sivakumar 2013).

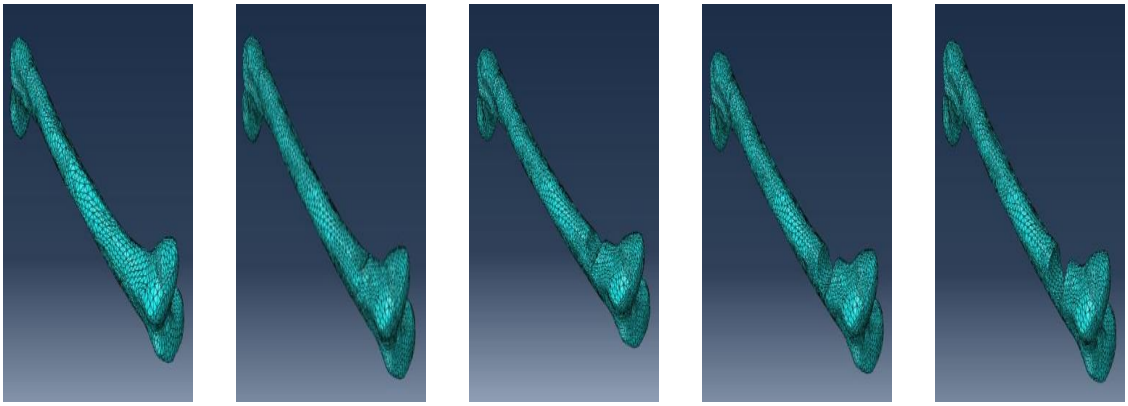

Model (I) Model (II) Model (III) Model (IV) Model (V)

Fig. 3 Three-dimensional approximated meshed models for femur bone with defect.

3. Methodology

In order to model the femur bone, Materialise Mimics software as an image processing software for three-dimensional design and modeling with the biomechanical application is used. The CAD software is not a perfect tool for modeling the femur bone as the bone has a complex geometrical shape, with complex surfaces and boundaries but Materialise Mimics software models the geometry using splines, which is suitable for having FE simulation (Bhardwaj *et al*. 2014, Tse *et al*. 2015). Then, SOLIDWORKS software is used for better producing the defects in femur bone. The length of the bone is assumed to be 0.45 m which is intended for men aged 27 years old with height 173 cm and women aged 24 years old with height 169 cm and the idea of geometry and size of the defect is coming from the work of (Amanatullah *et al*. 2014) although the defects modeled in the present paper are not the same as their modeling. These defects can be seen in part (b) of Fig. 2.

Then the ABAQUS software is adopted to study the vibration of femur bones with cortical defects using the finite element method. The finite element method is widely accepted and used as an alternative tool for biomechanics modeling which has complicated geometrical shapes and heterogeneous material properties (Mow *et al*. 1993, Gupta and Tse 2014).

Meshed models of femur bones with different types of defects are shown in part (c) of Figs. 2 and 3. The meshed model consists of 131726 quadratic tetrahedral elements of type C3D10 with 192028 nodes. The global size of meshes, is about 0.004 m. It is important to note that the convergence of results is also checked in some cases. It is noted that the geometry of defects is defined in Fig. 4.

4. Numerical results

In the first part of this section, the natural frequencies of femur bone with defects are presented. In order to show the accuracy of present modeling, our results are compared with those available in the literature in Table 1. A great agreement between the results is achieved. As the next step, in order to present the results of femur bone, the material properties are classified into two different models, as shown in Fig. 5. One of them is the isotropic model with Young's modulus E=17 GPa, the mass

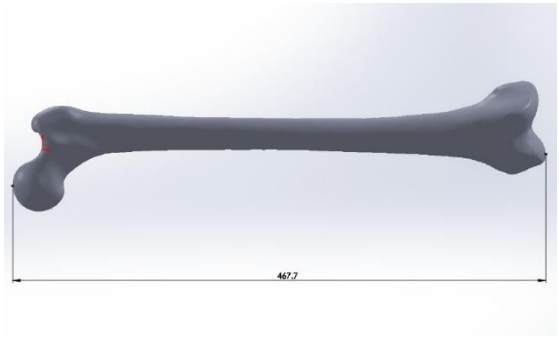

Model (I)

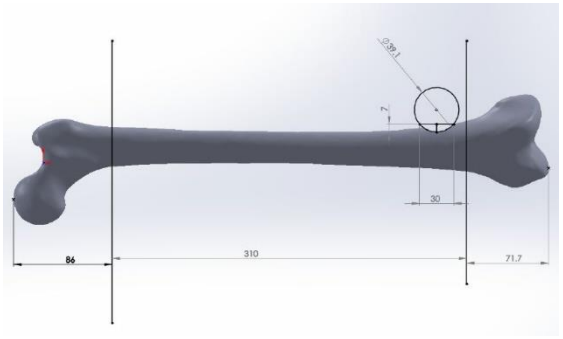

Model (II)

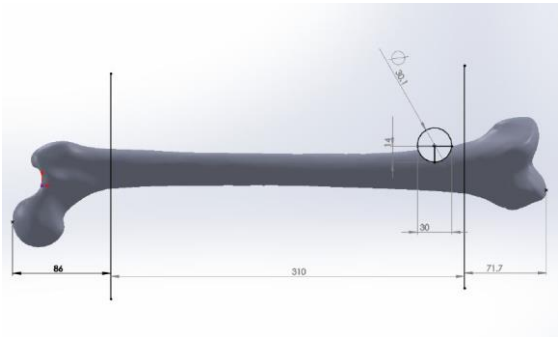

Model (III)

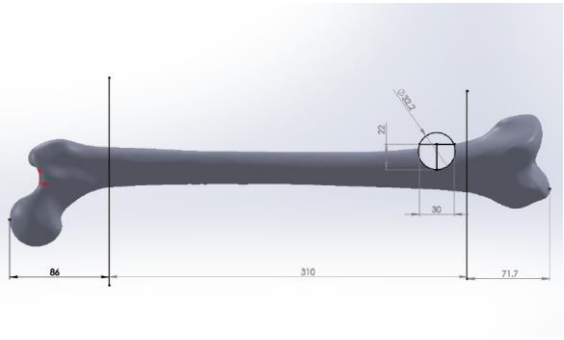

Model (IV)

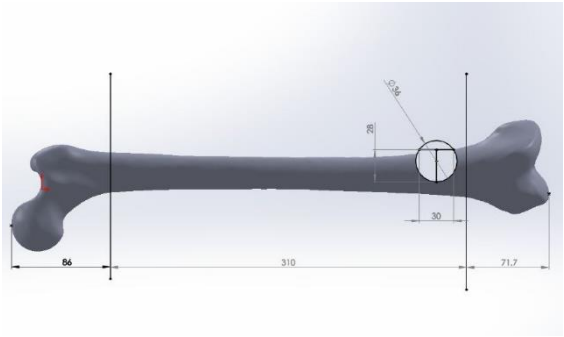

Model (V)

Fig. 4 Geometry of femoral defects.

density ρ=2132.6 kg/m^3, the Poisson's ratio υ=0.3 (Huang *et al*. 2012). In another model consisted of a cortical shaft along the bones' diaphysis and two cancellous parts in the two ends of bone which is closer to the material properties of real human bone. The cortical part is the same as the first model and the properties of the cancellous parts are E=3390 GPa, the mass density ρ=1100 kg/m^3, the Poisson's ratio υ=0.3 (Hodgskinson and Currey 1992, Jade 2012). From our results, one may find that the results of the first model are not accurate in comparison with the second model and the isotropic model should not be used.

In Table 2, the natural frequencies of femur bone with different types of defects for two different material properties are tabulated. In this table, it is assumed that the bone has the simply supported boundary condition as shown in Fig. 6. For this example, the highest value of 500.19 Hz is observed

Table 1 A compression study between analytical method and present simulation for the first four natural frequencies (Hz) of beam

Type of section	Boundary Condition	Mode number	Exact Solution	Present
Rectangular Section	Fix-Fix	1	1.4525	1.4528
		2	4.0009	4.0013
		3	7.8461	7.8352
		4	12.969	12.933
	Fix-Free	1	0.2282	0.2284
		2	1.4265	1.4307
		3	4.0009	4.0028
		4	7.8461	7.8349
Circular Section	Fix-Fix	1	2.5209	2.5131
		2	6.9437	6.9101
		3	13.617	13.501
		4	22.508	22.223
	Fix-Free	1	0.3961	0.3955
		2	2.4758	2.4755
		3	6.9437	6.9160
		4	13.617	13.509

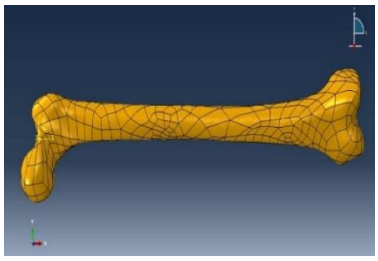

(a) Model 1

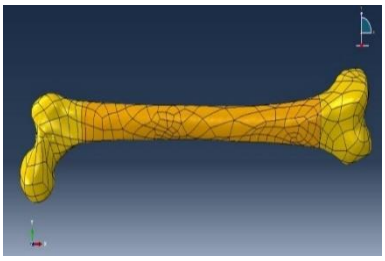

(b) Model 2

Fig. 5 Approximated models for the material properties of femur bone: a) isotropic model, b) non-homogeneous model consisted of a cortical shaft and two cancellous parts.

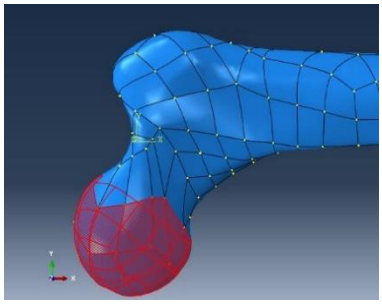

(a) Model 1

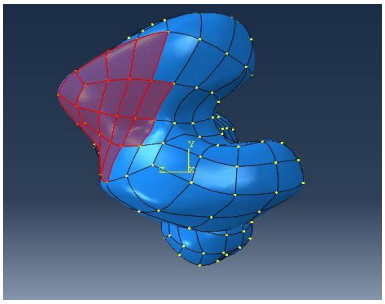

(b) Model 2

Fig. 6 Boundary conditions for femur bone based on the human skeleton

in the case of the isotropic bone for the first mode of vibration and the highest value of 332.01 Hz is seen in the of the bone model consisted of a cortical shaft and two cancellous parts. Besides, the highest value in all modes of vibration is 3374.9 Hz for the isotropic model and 2636.2 Hz for the

Table 2 Natural frequencies (Hz) of femur bone with defects including isotropic and non-homogeneous models

Mode	Model (I)		Model (II)		Model (III)		Model (IV)		Model (V)	
	Model 1	Model 2	Model 1	Model 2	Model 1	Model 2	Model 1	Model 2	Model 1	Model 2
1	500.19	332.01	497.80	331.71	485.47	330.55	467.60	325.15	436.13	314.65
2	572.74	371.48	570.90	371.61	563.55	372.25	554.89	372.26	537.52	369.49
3	1210.1	865.85	1211.5	866.70	1213.8	868.89	1212.9	868.26	1172.8	859.03
4	1355.7	1047.6	1351.8	1049.4	1327.7	1055.4	1281.8	1058.7	1180.8	1025.3
5	1897.4	1331.9	1897.6	1331.3	1883.6	1315.3	1840.6	1219.9	1586	1112.8
6	2055.2	1530.7	2050.1	1522.3	2013.1	1472.2	1935.2	1347.6	1770	1180.8
7	2422.1	1843.2	2421.1	1840.3	2404.3	1825.4	2357.9	1772.1	2231.5	1684.6
8	2921.8	2099.9	2918.7	2102.6	2869.6	2114.5	2757	2143.1	2586.1	2133.3
9	3023.1	2231.4	3028.8	2240.7	3045.9	2257.5	3043.5	2252.2	2860.8	2218.4
10	3374.9	2636.2	3359.2	2632.9	3278.4	2610.8	3194.9	2538.5	3199	2436.6

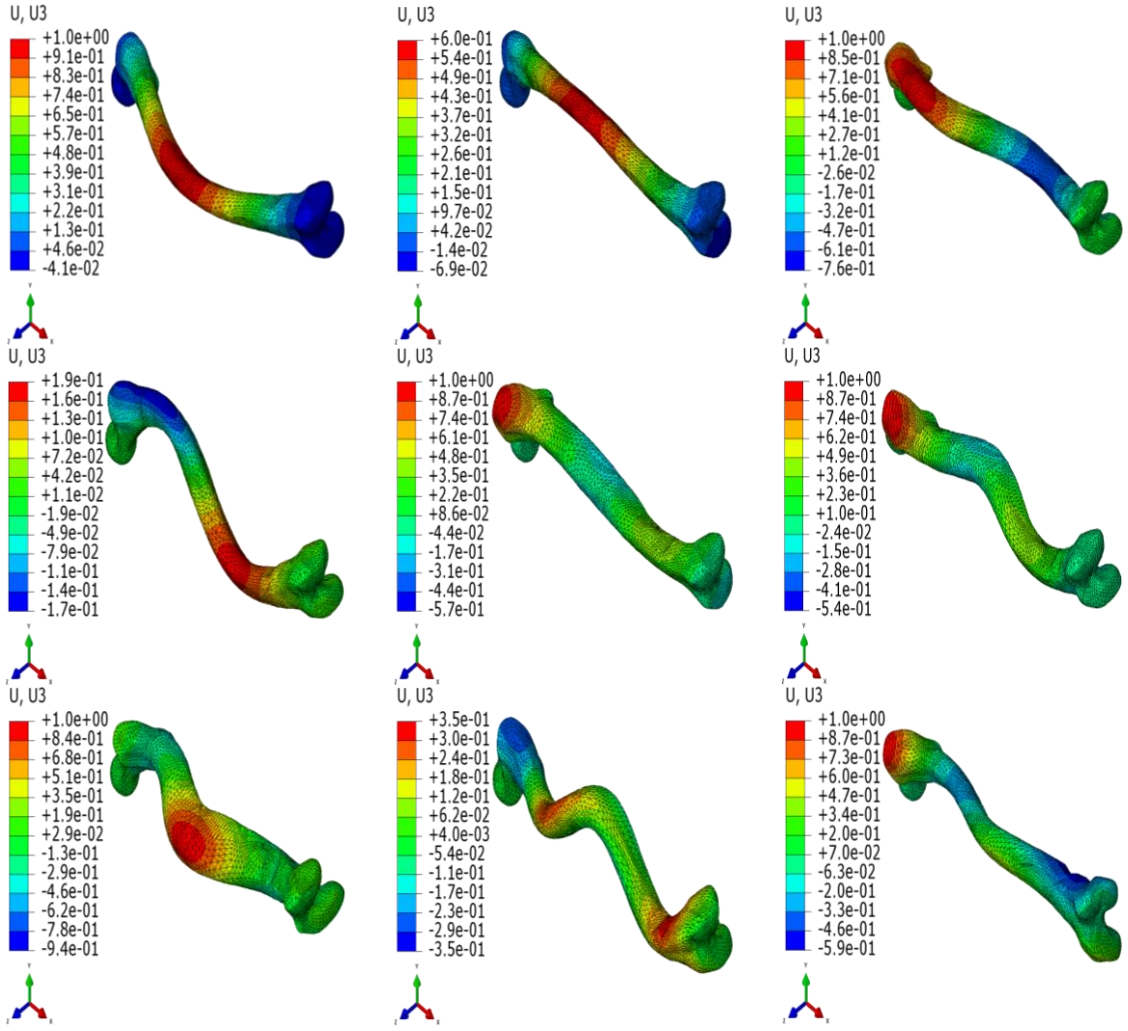

Fig. 7 First nine modes of vibration for femur with a defect.

Table 3 A compression study between analytical method and present simulation for buckling load ($\times 10^6$) N of beam

Type of section	Boundary Condition	Exact Solution	Present
Rectangular Section	Fix-Fix	3.7899	3.7747
	Fix-Free	0.2369	0.2368
Circular Section	Fix-Fix	3.0372	3.0270
	Fix-Free	0.1898	0.1898

Table 4 Buckling loads (N) of femur bone with defects including isotropic and non-homogeneous models

Mode	Model (I)		Model (II)		Model (III)		Model (IV)		Model (V)	
	Model 1	Model 2	Model 1	Model 2	Model 1	Model 2	Model 1	Model 2	Model 1	Model 2
1	5614.6	3055.5	5693	3561.3	5391.4	2947.5	5691.6	2751	3979	2302.7
2	6524	3507.8	6669.7	4101.6	6632.7	3460	7142.5	3446.6	5693.9	3101.7
3	10080	6876.9	10284	8066.6	10235	6832	11434	6758.5	9038.2	5808.7
4	11295	7133.2	11609	8454.2	11831	7018.8	13476	6933.3	11390	5904.8
5	19216	7215.8	19610	8622	19535	7136.7	21417	7131.4	12873	6210.8
6	21100	8335.2	21676	9802.5	22007	7722.3	24435	7468.2	17207	6463.3
7	25787	8459.2	26188	9917.7	25532	7979.6	26972	7712	17893	6695.3
8	27106	8948.4	27853	10515	28322	8931.4	28345	8631.6	18643	7497.5
9	28537	9197.2	29066	10585	29073	9352.4	29045	9043.5	19513	7846.5

second model.

From this table, it is found that in some cases the femoral defect plays an important role in the vibration of femur bone and its effect can't be neglected. It is also understood that for almost all modes of vibration presented in this table, the isotropic model doesn't have acceptable results. This table shows that all the natural frequencies predicted by model 2 are less than those calculated based on model 1. It is mentioned that the external excitation on the femur bone must be avoided to coincide with these natural frequencies; otherwise, it could lead to fracture of the bone (Gupta and Tse 2014).

The first-nine modes of vibration for femur bone with the are also shown in Fig. 7. The sub-figures show the displacement profile for the vibration at the corresponding modal frequency. It is noted that the buckling analysis of bones with femoral defects is also done by the authors of the paper but the results have some negative critical buckling loads and some variations can be seen in the results which may not agree with engineering sense. So, we decide to omit the buckling results. We think that the complexity of bone geometry with defect, the nodes selected for boundary condition and the meshes used in it may cause this problem. A bit of this problem may be seen in Table 4 where as some of the frequencies of model (II) are less than those in model (I).

At this step, we are going to study the results of the stability analysis of femur bones with femoral defects for isotropic and non-homogeneous models. Both buckling loads and modes of buckling are presented in this part. As the first step, a comparison between the critical buckling loads for different boundary conditions are presented in Table 3. It can be seen that our results are in good agreement with those in the open literature. Before starting our discussion on femur bone, similar to the previous part, the boundary conditions are introduced. As shown in Fig. 8, the boundary conditions on both sides of the femur bone are defined. For the left sub-figure, all the

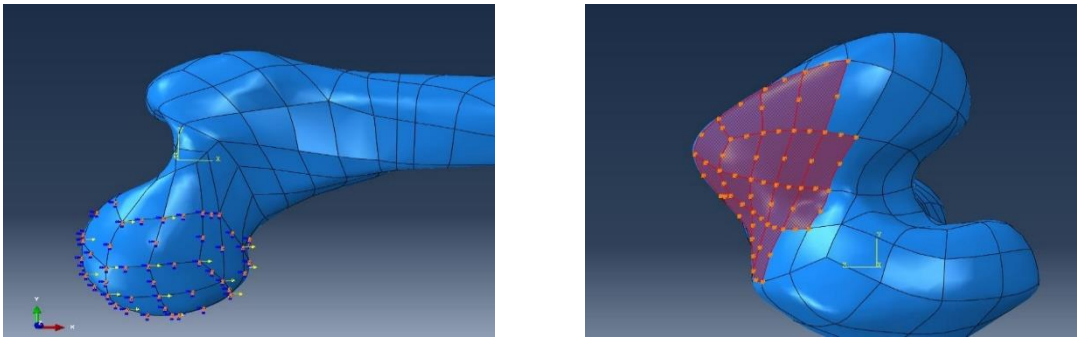

(a) Model 1 (b) Model 2

Fig. 8 Boundary conditions used in our modeling

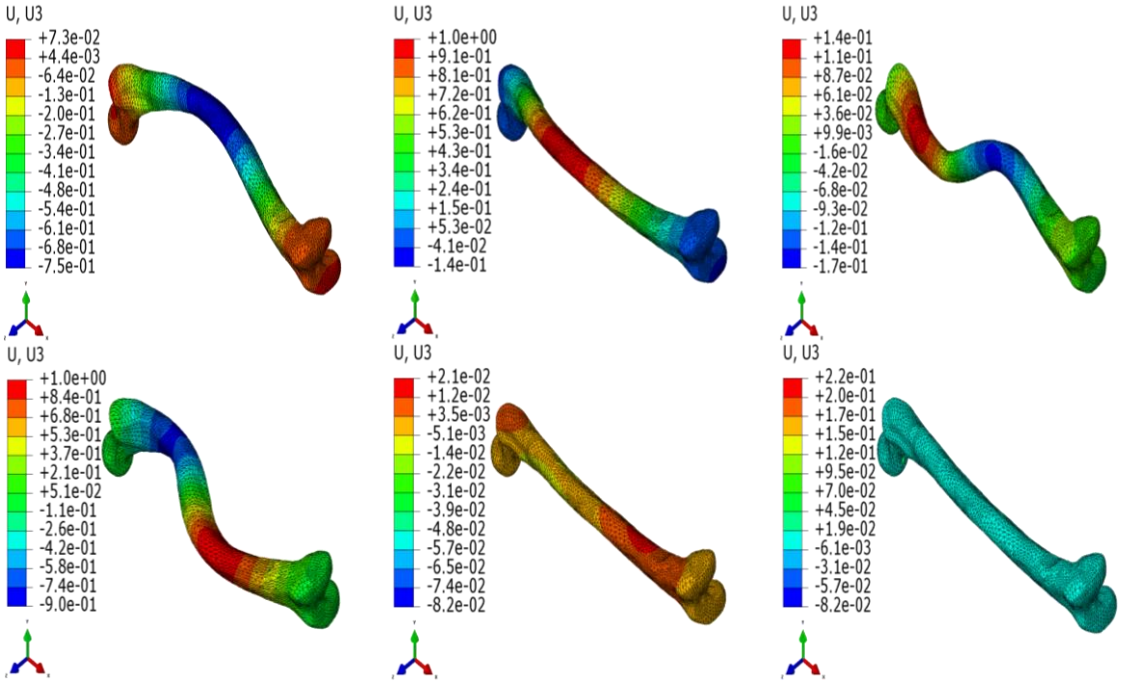

Fig. 9 First six modes of buckling for femur bone with a defect.

degrees of freedom except the displacement in the x-direction are restrained and for the right sub-figure, the pinned boundary condition introduced in ABAQUS software is used. It is noted that for the start of buckling analysis, 1N load is applied at the end hip joint of femur bone (left sub-figure). The results of buckling loads for the femur bones with different types of defects for both isotropic and non-homogeneous models are tabulated in Table 4 and the modes of buckling are shown in Fig. 9 for the first 6 modes of buckling. One key result from this table is that types of femoral defects and the non-homogeneous behaviors of femur bones play an important role in the stability of them.

From this table, it is seen that for both isotropic and non-homogeneous models, the Model V of femoral defects has the lowest critical buckling load as it is expected from its geometrical shape. It is important to mention that our engineering sense tells us that the Model I of defects should have

the highest critical buckling load but it does not occur. This may be because of the meshing process for bones because of their complicated shapes. According to the above note, it worth noting that in some steps in our modeling, we even reach the negative buckling loads. All in all, it seems that strange behaviors of buckling loads can raise some questions for future works. At the end of this section, it is recommended for other researchers to study the stresses in femur bones with cortical defects which can be useful for predicting or preventing accidental fracture of femur bone. Moreover, the fracture location can also be predicted from the stress contours (Bhardwaj *et al*. 2014).

5. Conclusions

In this article, 3D modeling of femur bones with femoral defects was presented using Materialise Mimics software, SOLIDWORKS software and ABAQUS software. A major strength of this study was the modeling of defects in femur bones. For different types of femoral defects, the natural frequencies and buckling loads were calculated and the modes of vibration and buckling were proposed. From our results, it may be found that in some cases, the femoral defect plays an important role in the vibration and stability of femur bone and their effects should be considered. Moreover, a non-homogeneous model for the material properties of femur bones were presented. The idea was that, unlike some papers that attribute one type of material property to all parts of bone, the bone divided into two parts. The two ends have the cancellous properties and the shaft considers cortical bone. This non-homogeneous model seemed to have more accuracy in comparison with the isotropic model although there are some drawbacks to our proposed model. For example, according to figure 5, it looks like it was better that we finished the cancellous part at the neck of bone.

References

Amanatullah, D.F., Williams, J.C., Fyhrie, D.P. and Tamurian, R.M. (2014), "Torsional properties of distal femoral cortical defects", *Orthopedics*., **37**(3), 158-162. https://doi.org/10.3928/01477447-20140225-51.

Anderson, D.E. and Madigan, M.L. (2013), "Effects of age-related differences in femoral loading and bone mineral density on strains in the proximal femur during controlled walking", *J. Appl. Biomech*., **29**(5), 505-516. https://doi.org/10.1123/jab.29.5.505.

Belaid, D., Germaneau, A., Bouchoucha, A., Brémand, F., Brèque, C., Rigoard, P. and Vendeuvre, T. (2017), "Finite element analysis of mechanical behavior of stabilization techniques for tibial plateau fractures", *Comput. Meth. Biomech. Biomed. Eng*., **20**(S1), 13-14. http://dx.doi.org/10.1080/10255842.2017.1382837.

Bhardwaj, A., Gupta, A. and Tse, K.M. (2014'), "Mechanical response of femur bone to bending load using finite element method", *2014 Recent Advances in Engineering and Computational Sciences (RAECS)*, 1-4.

Campion, D., Dakhil, N., Llari, M., Evin, M., Mo, F., Thefenne, L. and Behr, M. (2017), "Finite element model of a below-knee amputation: a feasibility study", *Comput. Meth. Biomech. Biomed. Eng*., **20**(S1), 35-36. http://dx.doi.org/10.1080/10255842.2017.1382848.

Coquim, J., Clemenzi, J., Salahi, M., Sherif, A., Tavakkoli Avval, P., Shah, S., Schemitsch, E.H., Bagheri, Z.S., Bougherara, H. and Zdero, R. (2018), "Biomechanical analysis using FEA and experiments of metal plate and bone strut repair of a femur midshaft segmental defect", *BioMed Res. Int*., **2018**, Article ID 4650308, 11. https://doi.org/10.1155/2018/4650308.

El Sallah, Z.M., Smail, B., Abderahmane, S., Bouiadjra, B.B. and Boualem, S. (2016), "Numerical simulation of the femur fracture under static loading", *Struct. Eng. Mech*., **60**(3), 405-412. http://dx.doi.org/10.12989/sem.2016.60.3.405.

Geraldes, D.M. and Phillips, A.T. (2014), "A comparative study of orthotropic and isotropic bone adaptation

in the femur", *Int. J. Numer. Meth. Biomed. Eng*., **30**(9), 873-889. https://doi.org/10.1002/cnm.2633.
Gupta, A. and Tse, K. (2014), "Vibration analysis of femur bone using Elmer", *J. Eng. Sci. Technol, Speial Issue on ICMTEA Conference*, December.
Haider, I.T., Speirs, A.D. and Frei, H. (2013), "Effect of boundary conditions, impact loading and hydraulic stiffening on femoral fracture strength", *J. Biomech*., **46**(13), 2115-2121. https://doi.org/10.1016/j.jbiomech.2013.07.004.
Hambli, R. (2014), "3D finite element simulation of human proximal femoral fracture under quasi-static load", *Adv Bioeng Appl*., **1**(1), 1-14. https://doi.org/10.12989/aba.2013.1.1.001.
Hodgskinson, R. and Currey, J. (1992), "Young's modulus, density and material properties in cancellous bone over a large density range", *J. Mater. Sci.: Mater. Medicine*., **3**(5), 377-381. https://doi.org/10.1007/BF00705371.
Huang, B., Chang, C., Wang, F., Lin, A., Tsai, Y., Huang, M. and Tseng, J. (2012), "Dynamic characteristics of a hollow femur", *Life Sci. J*., **9**(1), 723-726.
Jade, S. (2012), "Finite element analysis of a femur to deconstruct the design paradox of bone curvature", Masters Theses, University of Massachusetts Amherst.
Kumar, A., Garg, T. and Patil, P.P. (2014), "Free vibration modes analysis of femur bone fracture using varying boundary conditions based on FEA", *Procedia Mater. Sci*., **6**, 1593-1599. https://doi.org/10.1016/j.mspro.2014.07.142.
Ma, L., Zhou, Y., Zhang, Y., Zhou, X., Yao, Z., Huang, W., Qiao, G. and Xia, H. (2014), "Biomechanical evaluation with finite element analysis of the reconstruction of femoral tumor defects by using a double-barrel free vascularized fibular graft combined with a locking plate", *Int. J. Clinic. Exper. Medicine*., **7**(9), 2425.
Mahmoud, S.R., Tounsi, A., Ali, A.T. and Al-Basyouni, K.S. (2014), "The effect of initial stress and magnetic field on wave propagation in human dry bones", *Bound. Value Prob*., **2014**(1), 135. https://doi.org/10.1186/1687-2770-2014-135.
Mow, V.C., Ateshian, G.A. and Spilker, R.L. (1993), "Biomechanics of diarthrodial joints: a review of twenty years of progress", *J. Biomech. Eng*., **115**(4B), 460-467. https://doi.org/10.1115/1.2895525.
Nishiyama, K.K., Gilchrist, S., Guy, P., Cripton, P. and Boyd, S.K. (2013), "Proximal femur bone strength estimated by a computationally fast finite element analysis in a sideways fall configuration", *J. Biomech*., **46**(7), 1231-1236. https://doi.org/10.1016/j.jbiomech.2013.02.025.
Sadeghi, R., Bakhtiari-Nejad, F. and Goudarzi, T. (2018'), "Vibrational analysis of human femur bone", *ASME 2018 International Design Engineering Technical Conferences and Computers and Information in Engineering Conference*.
San Antonio, T., Ciaccia, M., Müller-Karger, C. and Casanova, E. (2012), "Orientation of orthotropic material properties in a femur FE model: A method based on the principal stresses directions", *Med. Eng. Phys*., **34**(7), 914-919. https://doi.org/10.1016/j.medengphy.2011.10.008.
Sivakumar, V. (2013), "Non-linear 3D finite element analysis of the femur bone".
Taylor, W., Roland, E., Ploeg, H., Hertig, D., Klabunde, R., Warner, M., Hobatho, M., Rakotomanana, L. and Clift, S. (2002), "Determination of orthotropic bone elastic constants using FEA and modal analysis", *J. Biomech*., **35**(6), 767-773. https://doi.org/10.1016/S0021-9290(02)00022-2.
Tse, K.M., Tan, L.B., Lim, S.P. and Lee, H.P. (2015), "Conventional and complex modal analyses of a finite element model of human head and neck", *Comput. Meth. Biomech. Biomed. Eng*., **18**(9), 961-973. https://doi.org/10.1080/10255842.2013.864641.
Voo, L., Armand, M. and Kleinberger, M. (2004), "Stress fracture risk analysis of the human femur based on computational biomechanics", *Johns Hopkins APL Tech Dig*., **25**(3), 223-230.
Yosibash, Z., Mayo, R.P. and Milgrom, C. (2014), "Atypical viscous fracture of human femurs", *Adv. Biomech. Appl*., **1**(2), 77-83.